Numerical Evaluation of the Lattice Green Functions

KOMA Yoshiaki *

Abstract: The Green functions take the roles of propagators in quantum field theories, which provide information on the interaction between particles. We evaluate the Green functions for a massless boson defined on a three-dimensional Euclidean lattice numerically, and investigate the lattice effects by comparing the results with the continuum ones. We find an inevitable difference at very short distances quantified approximately by an exponential function.

Key Words: Green function, Propagator, Lattice formulation

1. Introduction

Revealing the properties of quantum field theories often requires numerical methods, and a lattice formulation of spacetime offers a powerful method for this purpose. In this formulation, field variables of a theory are treated as the site or link variables, which allows us not only to solve the field equations by using numerical algorithms but also to compute the partition function that contains the quantum effects by using the Monte-Carlo method. Only the caveat may be that the numerical results obtained in this way suffer from systematic errors due to finite cutoff and finite volume. This is because one cannot perform computation practically in infinite volume with infinitesimally small lattice spacing. Therefore, it is always important to control the lattice artifacts in the numerical results.

The evaluation of the Green functions defined on the lattice, which we call the lattice Green functions, may give some hints. The Green functions take the roles of propagators in quantum field theories, which provide information on the interaction between particles. For a massless boson, such as the photon in quantum electrodynamics, carrying momentum p_μ, the propagator is given by $1/p^2$ in the momentum representation, and the Fourier transform corresponds to the well-known Coulombic potential $\sim 1/r$. If one dares to compute the same propagator and potential on the lattice, however, the results could be different from those in the continuum and infinite volume limits in some respects. Thus, the comparison of the lattice results with the continuum ones that can be obtained analytically will be useful to expose the lattice artifacts.

*Division of Liberal Arts

In this report, we present part of our numerical results on the behavior of the lattice Green functions for a massless boson in three-dimensional Euclidean space both in finite and infinite volumes. We then compare these results with those in the continuum theory. We partially resort to the coordinate space method to evaluate the lattice Green functions in infinite volume as demonstrated in [1–3].

2. The lattice Green functions

The lattice Green function for a massless boson in infinite volume in the coordinate representation $G_\infty(x)$ is generally defined by the equation

$$\Delta G_\infty(x) = -\delta_{x0} , \tag{1}$$

where Δ denotes the lattice Laplacian and δ_{x0} is the Kronecker delta, $\delta_{x0} = 1$ for $x = 0$ and $\delta_{x0} = 0$ for $x \neq 0$. In the N-dimensional Euclidean space, the left-hand side of Eq. (1) is written as

$$\begin{aligned}\Delta G_\infty(x) &= \sum_{\mu=1}^{N} \nabla_\mu^* \nabla_\mu G_\infty(x) \\ &= \sum_{\mu=1}^{N} [G_\infty(x+\hat{\mu}) + G_\infty(x-\hat{\mu}) - 2G_\infty(x)] ,\end{aligned} \tag{2}$$

where ∇_μ and ∇_μ^* are the forward and backward differences to a direction μ, respectively. The lattice spacing is set to one throughout this report.

The solution of Eq. (1) is formally obtained by performing the Fourier transformation of the Green function in the momentum representation. On the lattice, momentum carried by a particle is defined by

$$\hat{p}_\mu = 2 \sin \frac{p_\mu}{2} , \tag{3}$$

where $p_\mu \in [-\pi, \pi]$. With this lattice momentum the Green function in the momentum representation is given by

$$\tilde{G}_\infty(p) = \frac{1}{\hat{p}^2} = \frac{1}{4 \sum_\mu \sin^2 \frac{p_\mu}{2}} = \frac{1}{2N - 2 \sum_\mu \cos p_\mu} , \tag{4}$$

and the Fourier transform is

$$G_\infty(x) = \int_{-\pi}^{\pi} \frac{d^N p}{(2\pi)^N} e^{ipx} \tilde{G}_\infty(p) \ , \tag{5}$$

where $p\,x = \sum_{\mu=1}^{N} p_\mu x_\mu$.

In finite volume with periodic boundary conditions in all directions, p_μ in Eq. (3) is discretized as $p_\mu = 2\pi n_\mu / L_\mu$ with integers $n_\mu = 0, 1, 2, ..., L_\mu - 1$. The Green function in the momentum representation is then given by

$$\tilde{G}_L(p) = \frac{1}{\hat{p}^2} = \frac{1}{4\sum_\mu \sin^2 \frac{p_\mu}{2}} = \frac{1}{2N - 2\sum_\mu \cos \frac{2\pi n_\mu}{L}} \ , \tag{6}$$

and the Fourier transform is

$$G_L(x) = \frac{1}{V} \sum_{n_\mu \neq 0} e^{i \frac{2\pi n_\mu}{L_\mu} x_\mu} \tilde{G}_L(p) \ , \tag{7}$$

where $V = \prod_{\mu=1}^{N} L_\mu$. In order to avoid divide-by-zero computation, one may exclude the zero momentum mode $n_\mu = 0$ for all μ reluctantly, which yields a finite volume correction in Eq. (1) as

$$\Delta G_L(x) = -\delta_{x0} + \frac{1}{V} \ . \tag{8}$$

The Fourier transformation of $\tilde{G}_L(p)$ is easily achieved by using the FFT algorithm, while that of $\tilde{G}_\infty(p)$ needs subtle approach. One may rewrite Eq. (5) by using the modified Bessel functions I_n as

$$G_\infty(x) = \int_0^\infty d\alpha\, e^{-2N\alpha} \prod_{\mu=1}^{N} I_{x_\mu}(2\alpha) \ , \tag{9}$$

and evaluate this integral numerically. However, the convergence property of the integration depends on the spatial dimension N, since the modified Bessel function behaves as

$$I_n(2\alpha) \sim \sqrt{\frac{1}{4\pi\alpha}} e^{2\alpha} \tag{10}$$

for large α, where the integrand will be of $O(\alpha^{-2})$ for $N = 4$, $O(\alpha^{-3/2})$ for $N = 3$, and $O(\alpha^{-1})$ for $N = 2$. These asymptotic behaviors indicate that it may be difficult to obtain precise numerical values for lower dimensions $N \leq 3$ as the convergence is expected to be slow.

An interesting way to avoid the convergence problem is to use the coordinate space method as demonstrated in Refs. [1–3]. According to Ref. [1], the idea is based on Vohwinkel's observation that the lattice Green function satisfies a relation

$$(\nabla^*_\mu + \nabla_\mu) G_\infty(x) = x_\mu \int_{-\pi}^{\pi} \frac{d^N p}{(2\pi)^N} e^{ipx} \ln(\hat{p}^2) \ . \tag{11}$$

Summing over all directions μ in Eq. (11), one obtains sort of a recursion relation

$$G_\infty(x+\hat{\mu}) = G_\infty(x-\hat{\mu}) + \frac{2x_\mu}{\rho} \sum_{\nu=1}^{N} [G_\infty(x) - G_\infty(x-\hat{\nu})] \tag{12}$$

with $\rho = \sum_{\mu=1}^{N} x_\mu$ for $\rho \neq 0$.

In three dimension [2], the direct evaluation of Eq. (1) at the origin leads to

$$G_\infty(1,0,0) = G_\infty(\mathbf{0}) - \frac{1}{6} \ , \tag{13}$$

where $G_\infty(\mathbf{0}) = G_\infty(0,0,0)$. The same relation also applies to $G_\infty(0,1,0)$ and $G_\infty(0,0,1)$ due to cubic symmetry. Moreover, the combination of the Green functions,

$$\begin{aligned} k(n) &= (n-1)G_\infty(n,0,0) + 2nG_\infty(n,1,0) \\ &+ (n+1)G_\infty(n,1,1) - nG_\infty(n-1,0,0) \\ &- 2(n-1)G_\infty(n-1,1,0) - (n-2)G_\infty(n-1,1,1) \ , \end{aligned} \tag{14}$$

is found to be a constant of motion, satisfying $k(n+1) = k(n)$ for $n \geq 1$, and the behavior of the Green functions at $n \to \infty$ leads to $k(n) = 0$. By setting $n = 1$ in Eq. (14), one further obtains a relation

$$G_\infty(1,1,1) = \frac{1}{2}(G_\infty(\mathbf{0}) - 3G_\infty(1,1,0)) \ . \tag{15}$$

Likewise the Green functions at any distances can be expressed as

$$G_\infty(x) = r_1(x) G_\infty(\mathbf{0}) + r_2(x) G_\infty(1,1,0) + r_3(x) \ , \tag{16}$$

where $r_1(x)$, $r_2(x)$, and $r_3(x)$ are rational numbers determined recursively by using Eq. (12).

The two inputs $G_\infty(\mathbf{0})$ and $G_\infty(1,1,0)$ in Eq. (16) are also computed from the recursion relation itself. In Table 1, we show the values of $G_\infty(\mathbf{0})$ and $G_\infty(1,1,0)$ obtained by solving simultaneous equations for $G_\infty(n,0,0)$ and $G_\infty(n,1,0)$ at long distances $n \to \infty$, which are expected to behave as $G_\infty(n,0,0) \sim 1/(4\pi n)$ and $G_\infty(n,1,0) \sim$

Table 1: The $G_\infty(\mathbf{0})$ and $G_\infty(1,1,0)$ determined by setting the maximum number n.

n	$G_\infty(\mathbf{0})$
20	0.25273100985866300265128997805730657618044205557026865017
40	0.2527310098586630030260020266135700840185454806081835215
60	0.2527310098586630030260020266135701299925645074087004469
n	$G_\infty(1,1,0)$
20	0.0551914336877373167861103588492548550092182265478188015
40	0.0551914336877373170165449460300639096093757534683259826
60	0.0551914336877373170165449460300639378812455101391984498

$1/(4\pi\sqrt{n^2+1})$, respectively. Clearly, the values show convergence for large n. The presented values seem to be unnecessarily lengthy, but they should be as precise as possible in order to reduce accumulation of rounding errors during the numerical recurrence. If it is possible to perform computation with quadruple precision, the values determined at $n = 40$ can be used, where the difference of the lattice Green function from the continuum one at $n = 40$ is expected to be of $O(1/n^2) \sim 10^{-3}$. It is interesting to note that the value of $G_\infty(\mathbf{0})$ determined in this way agrees with the half of the Watson integral I_3 [4, 5],

$$G_\infty(\mathbf{0}) = \frac{I_3}{2} = \frac{\left(\sqrt{3}-1\right)\Gamma\left(\frac{1}{24}\right)^2\Gamma\left(\frac{11}{24}\right)^2}{192\pi^3} . \quad (17)$$

3. Numerical results

We shall present numerical results in three dimensions. In the continuum case, the Green function at the origin is divergent due to the $1/r$ behavior. In contrast, the lattice Green function at the origin is always finite both in finite and infinite volumes. In Fig. 1, we plot the values of $G_L(\mathbf{0})$ as a function of L, where the dotted line corresponds to $G_\infty(\mathbf{0})$. We find that $G_L(\mathbf{0})$ depends on the size L, which approaches $G_\infty(\mathbf{0})$ from below as the size L is increased.

In Fig. 2, we plot the on-axis lattice Green functions both in finite and infinite volumes, $G_L(r) \equiv G_L(r,0,0)$ and $G_\infty(r) \equiv G_\infty(r,0,0)$, which are compared with the continuum Green function $G(r) = 1/(4\pi r)$. The $G_\infty(r)$ seems to be identical to $G(r)$ except for the distances near the origin, while $G_L(r)$ are clearly different from $G(r)$ and are dependent on the size L. Although $G_L(r)$ approaches $G(r)$ gradually as the size L is increased, there still seems to be

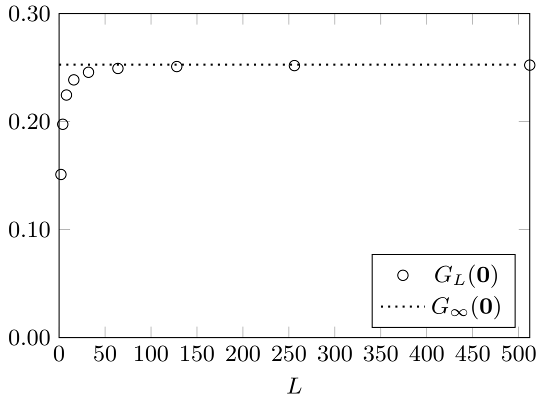

Fig. 1: The behavior of $G_L(\mathbf{0})$ as a function of L, which is compared with $G_\infty(\mathbf{0})$ (dotted line).

a constant gap even after taking the limit $L \to \infty$.

As shown in Fig. 3, however, we find that once the values at the origin are subtracted from the lattice Green functions, they seem to fall into one curve corresponding to $G(r) - G_\infty(\mathbf{0})$. We look at the difference between them carefully in Fig. 4, which clearly shows that the difference tends to disappear as the size L is increased. Only at very short distances for $r \le 5$ there is an inevitable difference. A chi-square fitting analysis for the infinite volume data indicates that the difference approximately obeys an exponential function

$$f(r) = 0.0151(3)e^{-0.84(2)r} . \quad (18)$$

In finite volume, Eq. (13) is modified to

$$G_L(1,0,0) = G_L(\mathbf{0}) - \frac{1}{6}(1 - \frac{1}{V}) , \quad (19)$$

where the finite volume correction originates from the removal of the zero momentum mode as already explained. Thus, the ratio of $G_L(1) - G_L(\mathbf{0})$ to $G_\infty(1) - G_\infty(\mathbf{0})$ is just given by $1 - 1/V$. For $L = 16$ it gives 0.9998, so that the relative error is only of 0.02 %.

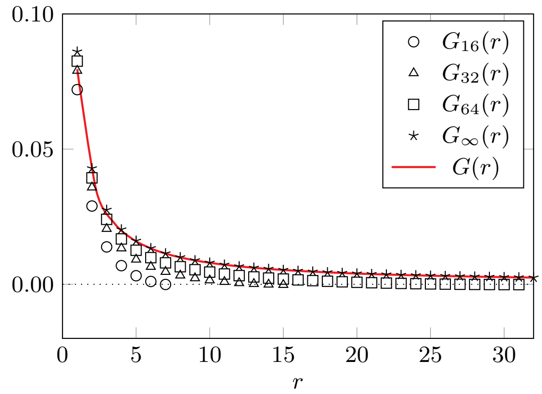

Fig. 2: The behaviors of the lattice Green functions $G_L(r)$ and $G_\infty(r)$, which are compared with the continuum Green function $G(r) = 1/(4\pi r)$.

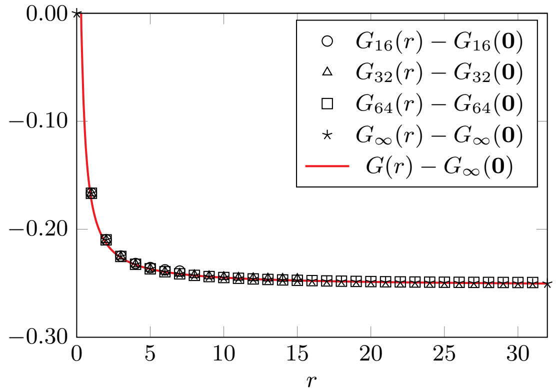

Fig. 3: The behaviors of the normalized lattice Green functions, where the values at the origin are subtracted.

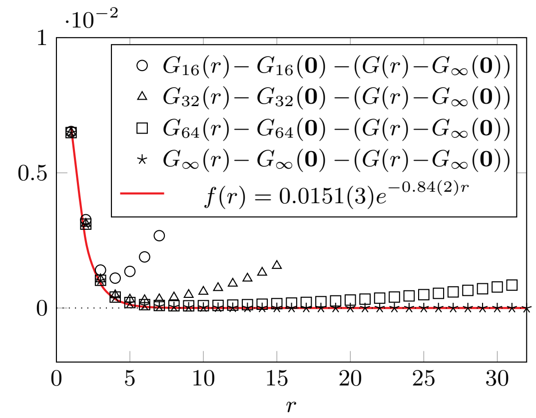

Fig. 4: The difference between the normalized lattice Green functions and the normalized continuum Green function.

Although analytical relations between $G_L(r) - G_L(\mathbf{0})$ and $G_\infty(r) - G_\infty(\mathbf{0})$ for $r \geq 2$ are not known yet, the results at small r in Fig. 4 indicate that the finite volume effect at short distances can easily be controlled. Whether or not one can control the finite volume effect at long distances depends on available computer resources. The results suggest that the size L should be taken at least four times larger than the distance of interest, since the effect of periodic boundary conditions appears around the distances of $L/4$.

On the other hand, the control of the finite cutoff effect as characterized by Eq. (18) may cause problem when one aims to clarify short-distance properties with massive particles. In a quantum field theory that the propagator is given by $1/(p^2 + m^2)$ with mass m, the Fourier transform corresponds to the Yukawa-type potential $\sim e^{-mr}/r$. In this case, the exponential function e^{-mr} certainly reflects a physical effect. What is complicated is that, in some of quantum field theories, masses are dynamically generated by the quantum effects. If this is the case, the discrimination of the finite cutoff effect is crucial, which will require systematic investigation including the scaling analysis.

4. Summary

We have investigated the lattice Green functions for a massless boson numerically both in finite and infinite volumes in three-dimensional Euclidean space. The presented results exhibit an inevitable difference from the continuum Green function at very short distances for $r \leq 5$, which is quantified by using an exponential function. Similar analyses can be performed also on the off-axis lattice Green functions. The control of the short-distance effect in our actual lattice computation [6] is in progress.

The author is grateful to Miho Koma for fruitful collaboration.

[1] M. Lüscher, P. Weisz, Nucl. Phys. B445 (1995) 429-450.
[2] S. Necco, R. Sommer, Nucl. Phys. B622 (2002) 328-346.
[3] D.S. Shin, Nucl. Phys. B525 (1998) 457-482.
[4] G.N. Watson, Quart.J.Math., Oxford 10 (1939) 266-276.
[5] G.S. Joyce, I.J. Zucker, Proc. Amer. Math. Soc. 133 (2005) 71-81.
[6] Y. Koma, E.-M. Ilgenfritz, T. Suzuki, and H. Toki, Phys. Rev. D64 (2001) 014015.